Pak. j. sci. ind. res. Ser. A: phy. sci. 2023 **66A**(2) 162-168

Optimization of ^{9}Be Target on Double Layer Beam Shaping Assembly (DLBSA) System to Increase the Intensity of Epithermal Neutron

Bilalodin*, Aris Haryadi, Kartika Sari and Farzand Abdullatif
Department of Physics, Faculty of Mathematics and Natural Science,
Jenderal Soedirman University, Indonesia

(received February 03, 2022; revised April 20, 2022; accepted June 24, 2022)

Abstract. The optimization of the ^{9}Be target has been carried out to increase the fast neutron flux and is expected to induce an increase in the epithermal neutron flux. Optimization was carried out by interacting of the ^{9}Be target with protons of 5-30 MeV and studying the effect of variations in the thickness and diameter of the target on the production of fast neutrons. Proton energy optimization results show that the interaction of a 30 MeV proton with a ^{9}Be target produces the highest fast neutron flux with an energy above 10 keV. The optimization results of the Be configuration results in 7 cm thick and 5 cm diameter capable of producing the highest fast neutron flux of 10^{13} cm^2/s. The increase in the fast neutron flux produced by the target resulted in an increase in the epithermal neutron flux from 1 x 10^9 n/cm^2/s to 4.26 x 10^9 n/cm^2/s.

Keywords: optimization, ^{9}Be target, DLBSA, fast neutron, epithermal neutron

Introduction

Boron Neutron Capture Therapy (BNCT) is a method of cancer therapy that utilizes capture reaction of thermal neutrons by ^{10}B atoms. BNCT has long been aspired to be an innovative form of radiation therapy that has the potential to treat various types of cancer. The success of the BNCT method depends on the ability to deposit ^{10}B compound selectively solely on cancer cells and the ability to irradiate thermal neutrons on their area (He *et al*., 2021).

Neutrons can be produced using an accelerator, one of which is a cyclotron. Cyclotron type accelerators have been largely developed in various countries including: the C-BENS, developed by the KURI Institute in Japan, the BNCT-based Accelerator (AB-BNCT), developed in Korea (Lee *et al*., 2020). Neutrons generated in the cyclotron system are obtained through the reaction of protons with target materials. However, the characteristics of the resulting neutrons do not allow them to be directly used because they also contain conta-minants apart from fast neutrons. Fast neutrons must be moderated using a beam shaping assembly (BSA) system (Hang *et al*., 2016; Savolainen *et al*., 2013).

BSA designs usually consist of a moderator, filter, reflector and collimator. Each component is typically designed using one type of material. However, the single layer configuration has its weakness, namely that each component of the BSA is not optimal in processing neutron radiation beams. Therefore, to overcome this weakness, a double layer model was developed using more than one material. Designing the BSA in a double layer configuration model allows better processing of the neutron source beam. The double layer beam shaping (DLBSA) model is optimized by components. Using step by step optimization, an epithermal neutron flux of 5 x 10^8 n/cm^2/s is produced (Bilalodin *et al*., 2020). When used as a neutron source in BNCT therapy, the value of the neutron flux is still relatively low. The low flux causes the therapy time to be long. Therefore, further optimization is still required, especially on the targets used in DLBSA in order to increase the epithermal neutron flux and consequently shorten the therapy time.

Several target materials have been investigated for larger neutrons production. The lithium (Li) target material is used to produce neutrons using low energy protons (< 5 MeV). A 100 (μm) thick Li is capable of producing fast neutrons of 1.4 x 10^{12} n/cm^2/s at its maximum with neutron energy of 1.8 MeV (Zaidi *et al*., 2017). Another material that was also tested was Beryllium (Be). The results showed that the interaction of 5 MeV protons beamed at a current of 2 mA produced a maximum fast neutron of 3.9 x 10^{12} n/cm^2/s (Hashimoto *et al*., 2014). The interaction of a proton of 30-40 MeV at a current

*Author for correspondence;
E-mail: bilalodin.unsoed@gmail.com

of 20 A with a Be target produces a maximum fast neutron of 1.0 x 10^{12} n/cm^2/s (Shin and Park, 2015).

In order for fast neutron flux to be able to produce an epithermal neutron flux of 10^9 n/cm^2/s after moderation in BSA, the number of fast neutrons produced from the interaction of protons with the target should be >1 x 10^{13} n/cm^2/s (Mank *et al*., 2011). When fast neutron flux produced is less than 10^{13} n/cm^2/s, the resulting epithermal neutron flux is low. Therefore, the right target configuration will contribute to the increase in the epithermal neutron flux. Suitable materials for target material include those with the characteristics of high thermal conductivity, not easily corroded and resulting short half-life radioisotope. The materials should also have high melting and boiling point characteristics, especially for targets that are reacted with high energy protons (Anderson *et al*., 2016). In this article, the results of the optimization of beryllium targets in DLBSA in producing fast neutrons will be presented and their effect on the increase of epithermal neutrons produced by DLBSA output.

Material and Methods

The target used in the Double layer beam shaping assembly (DLBSA) system is beryllium (Be), with mass number of 9. The target is bombarded by 30 MeV protons generated from a 30 MeV cyclotron type accelerator developed by the KURRI institute in Japan, namely C-BENS (Tanaka *et al*., 2011). The proton beam is designed to enter the cylinder through a vacuum tunnel which is 7 cm in radius and 20 cm in length. The target is placed at the end of the cylinder and placed in a wrapping chamber made of Ta alloy material. The reaction between Be and protons produces neutrons through the ^{9}Be(p,n)^{9}B reaction (Chavan *et al*., 2022). Neutron beam recording on target and DLBSA output is shown in Fig. 1.

Optimization of the target configuration was carried out by simulating protons with energy variations from 5 MeV to 30 MeV which ensure that the 30 MeV protons produce 10^{13} n/cm^2/s beam. The neutron flux conforms to the fast neutron beam standard for moderation into epithermal neutrons. The next step is to test its ability to produce fast neutrons. The test was carried out on variations in thickness and diameter of the target from 1 to 7 cm. In each test, the neutron yield spectrum, neutron flux distribution around the target and inside the DLBSA were calculated.

DLBSA is modelled as having four main components, namely moderator, reflector, collimator and filter. Each component is formed from a combination of two materials. The moderator is chosen from a combination of aluminium (Al) and BiF_2 materials. The reflector is selected from a combination of Pb material with FeC material. The collimator is composed of Ni and Borated polyethylene. At the final stage a combination of filters for fast neutron and thermal neutrons is selected. It is carried out by combining FeC with Cd materials, as a fast neutron and thermal neutron filter. Besides the Cd filters, a gamma filter made of Pb is installed (Bilalodin *et al*., 2019).

The design and recording of the characteristics of the neutron beam generated by the target and DLBSA was carried out using the Particle Heavy Ion Transport (PHITS) program version 3.2, with nuclear data JENDL-4.0 (Sato *et al*., 2013). In order to get simulation results with low statistical error, a large combination of maxcas and maxbch is carried out with a ratio of 10:1. The neutron beam produced by DLBSA is verified by calculating the neutron spectrum using Tally Track. The fast neutron dose rate and gamma dose is calculated by the Tally Track which is equipped with K_{fast} and K_{γ} conversion factors to convert flux into dose rate. The characteristics of the neutrons produced at the end of the DLBSA aperture are desired to meet the needs of BNCT according to the IAEA standards.

Results and Discussion

Profile of the neutron beam resulting from the interaction of proton and target. Figure 2 shows the neutron flux generated from bombardment of protons with 5 MeV to 30 MeV of energy on a beryllium (Be) target. Neutron flux as a function of projectile energy follows an exponential function at low energies and is linear at high energies. The difference in the curves at low and high energies is caused by the difference in the reactions that occur in the formation of neutrons. At low energies the formation of neutrons occurs through the Be(p,xn) reaction. In this reaction, one proton interacting with the target produces many neutrons. This results in an exponential curve, while at high energy, it follows the ^{9}Be(p,n)^{9}B reaction (Lee *et al*., 2020). The reaction shows that one proton produces one neutron, resulting in a linear curve.

The interaction of 30 MeV proton with ^{9}Be produces a boron isotope ^{9}B (Shin and Park, 2015). The boron

(^{9}B) isotope decays with a very short half life without emitting gamma rays (Stefanik *et al*., 2019; Capulat *et al*., 2014). The neutron flux at the energy of 30 MeV reaches 10^{13} n/cm^2/s. The value of the neutron flux is in accordance with the requirements to be moderated into epithermal neutrons.

The neutron flux resulting from the interaction of protons with the target Be yields neutrons or fast neutrons in the energy range of 10^{-2} to 10 MeV. The distribution pattern of the fast neutron energy produced by the interaction of protons with the target Be from 5 MeV to 30 MeV forms of a Gaussian distribution curve. The Gaussian curve shows that the energy of neutrons produce from the interaction of protons and targets varies randomly and continuously (Iwamoto *et al*., 2020). The simulation results also show that the Gaussian curve is higher as the energy of the protons reacting with the target is higher. This shows that the higher the proton energy, the more neutrons are produced. The spectral distribution curve of the interaction between protons and the target Be is shown in Fig. 3.

The interaction of protons with Be target produces fast neutrons. The highest fast neutron flux intensity is in the vicinity of the target (shown in red in Fig. 4). Low energy proton interaction results in a fast neutron flux around the target (Fig. 4). The higher the proton energy, the faster the neutrons spread through the moderator, reflector, collimator and still escape through the aperture. It shows that not all fast neutrons can be moderated by Al^{+} PbF_2 moderator and absorbed by FeCl fast neutron filter. The presence of fast neutrons that still escape the moderator is probably due to Aluminum (Al) as the main moderator is moderates mainly neutrons with energies between 10-100 keV (Ma *et al*., 2015). On the other hand, the second moderator PbF_2 containing element F, are only able to moderate neutrons below 1 MeV (Fantidis and Nicolaou, 2018). Based on the characteristics of the moderator used, the neutrons that still escape the moderation process are high energy neutrons above 1 MeV. Traces of fast neutrons begin to emerge from the target and spread throughout the DLBSA components, as shown in Fig. 4.

Effect of thickness and diameter of Be target on fast neutron production. The results of the optimization of the target configuration are shown in Figs. 5 and 6. The optimization was carried out with variations in

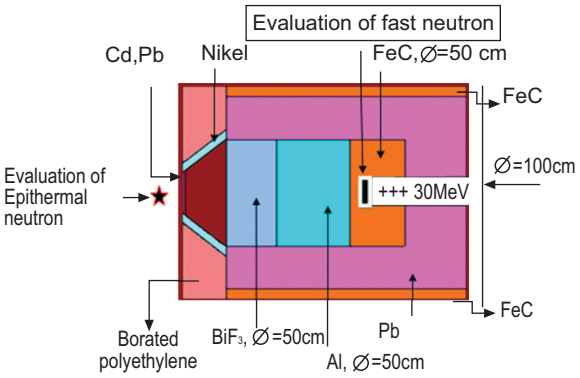

Fig. 1. Neutron beam recording on target and DLBSA output.

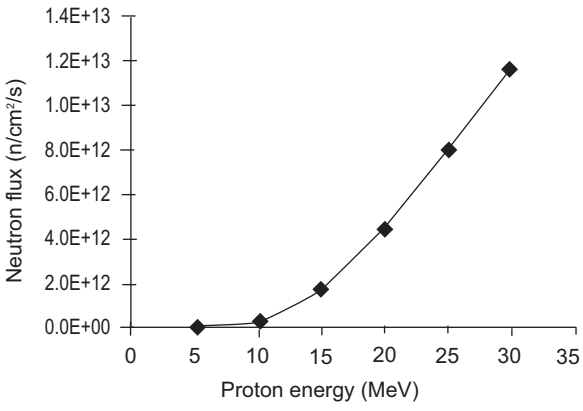

Fig. 2. Correlation of proton projectile energy with fast neutron flux.

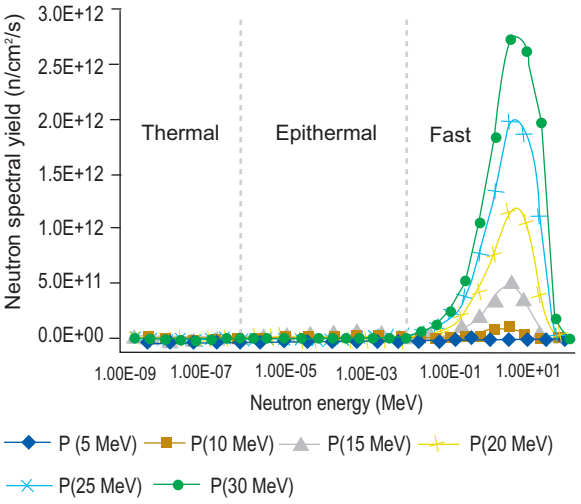

Fig. 3. Distribution curve of energy spectrum of neutrons resulting from the interaction between protons and the ^{9}Be target.

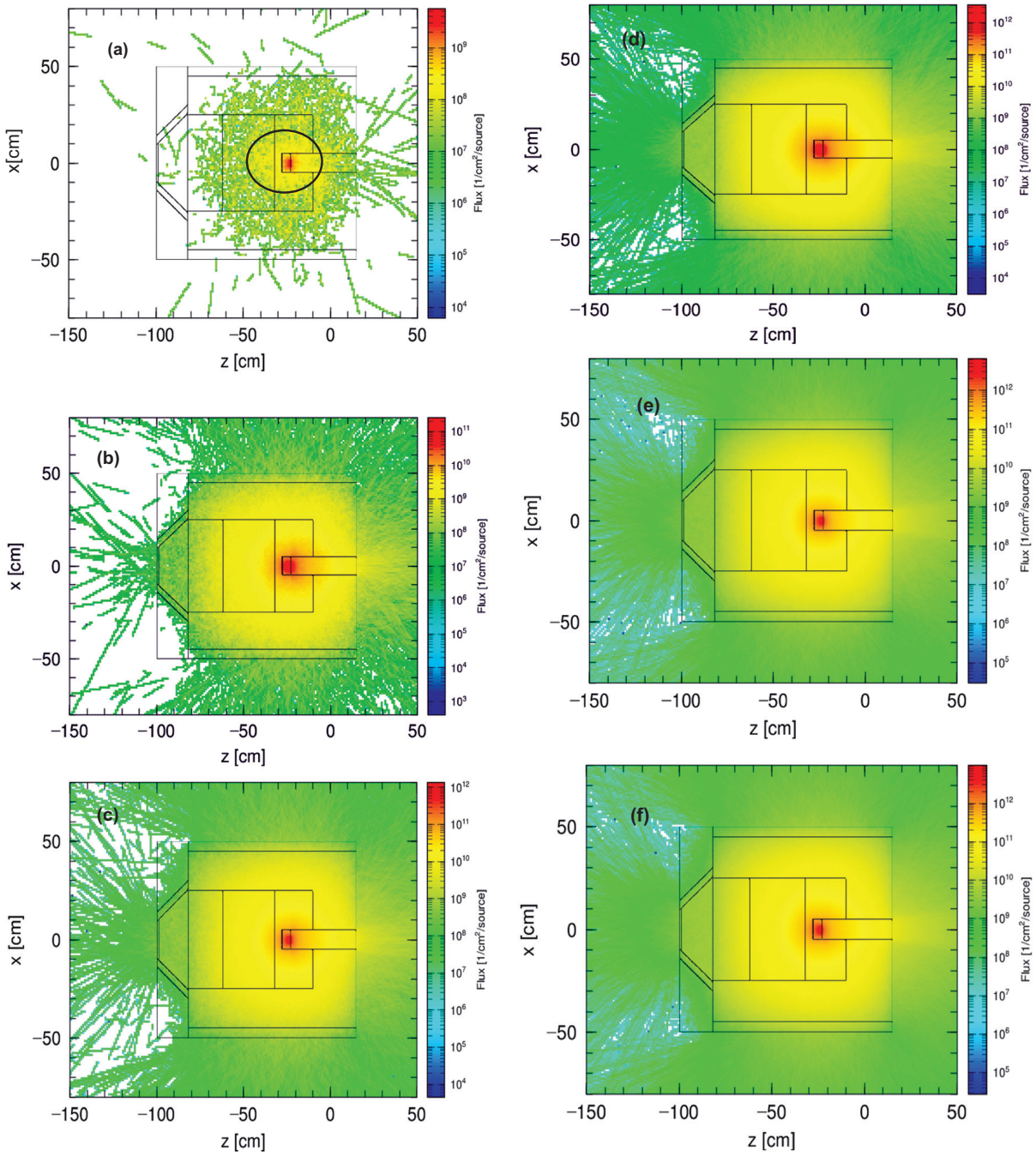

Fig. 4. Traces of fast neutrons resulting from interactions of proton around the target ^{9}Be and their distribution in the DLBSA. Proton energy **(a)** 5 MeV, **(b)** 10 MeV, **(c)**15 MeV, **(d)** 20 MeV, **(e)** 25 MeV **(f)** 30 MeV.

thickness and diameter to obtain the highest neutron flux. It gives a very significant increase in flux when the diameter of target is varied from 2 to 4 cm. The neutron flux reaches a constant value when the diameter changes from 4 to 7 cm. In general, the larger the diameter of the target, the greater the flux of fast neutrons produced. The larger the diameter of the target, the more is the interaction of protons with the target surface, thereby contributing to the increase in the neutron flux.

Based on the maximum neutron flux obtained from the variation of the target diameter, the thickness of the target is then varied. The simulation result shows that

the variation of the target thickness from 1 to 5 cm resulted in an increase in the neutron flux and the maximum is at 5 cm thick. The increase in neutron flux is caused by the increasing number of protons interacting with the target material, thus increasing the number of neutrons released from the metal Be. On the other hand, increasing thickness tends to decrease the fast neutron flux. The thicker the target, the more protons interact with the electrons on the target, thereby reducing the number of electrons produced (Feghhi *et al*., 2014).

The results of target optimization at a diameter of 7 cm and a thickness of 5 cm reached a fast neutron flux of 1.137 x 10^{13} n/cm^2/s. The magnitude of the neutron flux is sufficient to be moderated to epithermal neutrons greater than 1.0 x 10^9 n/cm^2/s (Mank *et al*., 2011).

Effect of Be target optimization on the increase of epithermal neutrons. The results of optimization of the target configuration for increasing epithermal neutrons are shown in Fig. 7. The neutron flux before optimization of the target configuration is 1.09 x 10^9 n/cm^2/s and after the optimization a total epithermal neutron flux of 4.26 x10^9 n/cm^2/s is obtained. The number of epithermal neutron flux using an optimized target is four times greater than using a nonoptimized target. The increase in the number of epithermal neutrons is caused by the increasing number of fast neutrons which can be reduced in energy to epithermal neutrons due to moderations in the DLBSA system. The process in which the energy of fast neutrons are reduced by a moderator into epithermal neutrons is inelastic collisions mechanisms (Koay *et al*., 2018).

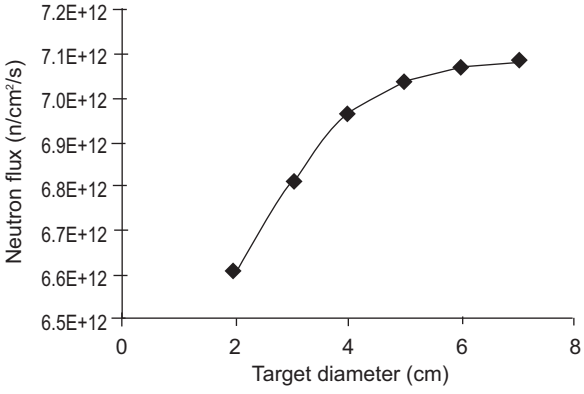

Fig. 5. Effect of variation target diameter on fast neutron flux.

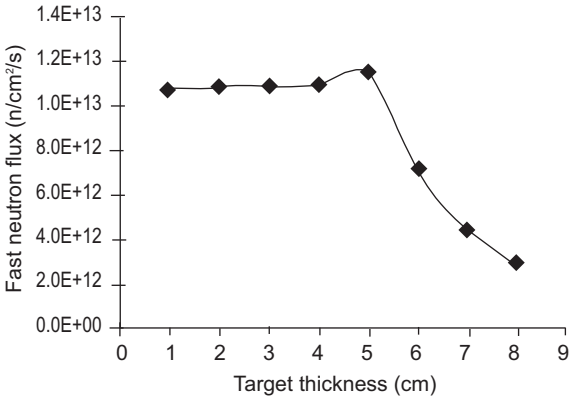

Fig. 6. Effect of changes in target thickness on fast neutron flux.

The spectral pattern produced by DLBSA is composed of thermal neutron flux, epithermal neutrons and fast neutrons. The neutron energy produced by DLBSA consists of thermal neutrons with energy less than 10^{-6} MeV, epithermal neutrons with energy range of 10^{-6} to 10^{-2} MeV and fast neutrons with energy more than 10^{-2} MeV. In the spectrum curve, the epithermal neutron value is the largest in percentage. This is indicated by a widening curve in the epithermal energy range of 10^{-6} to 10^{-2} MeV. Based on the figure, it can also be seen that the spectrum curve of the neutron beam tends to have a peak at the energy of 10^{-2} MeV. It shows that the neutron beam that exits at the end of the collimator (aperture) is dominantly in the form of epithermal neutrons.

The simulation result of the distribution of the epithermal neutron flux in the DLBSA is shown in Fig. 8. The

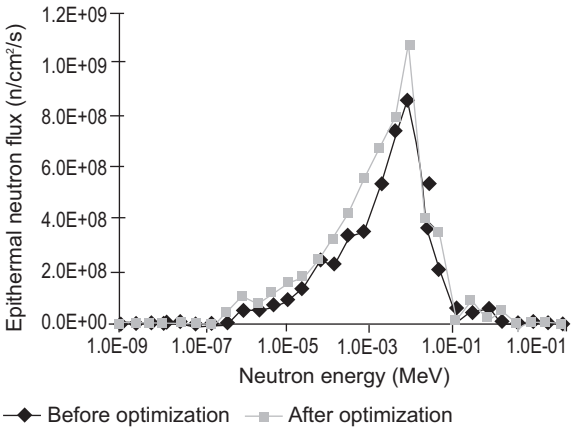

Fig. 7. Energy spectrum of epithermal neutrons generated by DLBSA before and after target optimization.

distribution of the epithermal neutron flux in the DLBSA is represented by colour. Low neutron flux intensities are depicted in blue and high intensities are shown in red. It can be seen from the figure that the epithermal neutron flux spreads out in the DLBSA. The intensity of the epithermal neutron flux is highest in the first filter with z=0 (shown in red) and increases through the moderator, collimator and decreases after passing through the filter with z >-100 (shown in yellow). The decrease in the epithermal neutron flux is deemed to be caused by the transformation of epithermal neutrons into thermal neutrons due to a collision with the material it passes through (Faghihi and Khalili, 2013). The epithermal neutron flux at the end of the collimator (aperture) >1.0 10^{9} n/cm^{2}/s.

Based on its characteristics, the epithermal neutron flux produced by the DLBSA source can be applied as the main neutron source for BNCT. The epithermal neutron flux intensity of 4.26 10^{9} n/cm^{2}/s can be used as a source for cancer therapy that operates for less than 1 h. Because the neutron flux of 1.0x10^{9} can be applied for 1 h for a maximum dose of 50 Gy (Copulat *et al*., 2014). The epithermal neutrons produced from DLBSA can be used as a neutron source for cancer therapy which is located 2-8 cm deep. Some types of cancer that may be treated using a neutron source are head and neck cancer, glioblastoma, lung cancer, breast cancer, pancreas, brain tumors and sarcomas (Dymoa *et al*., 2020).

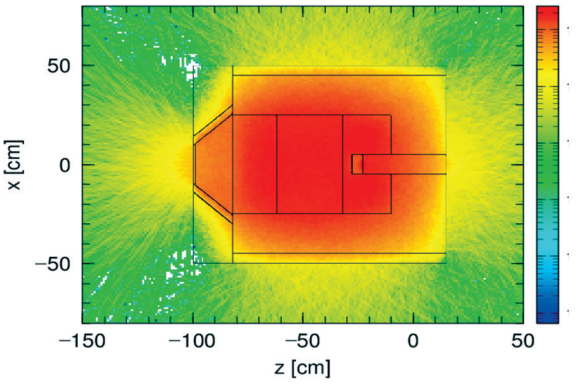

Fig. 8. Distribution of epithermal neutron flux in the DLBSA system. x represents the width and z represents the length of the DLBSA.

Conclusion

The interaction of 5-30 MeV protons with ^{9}Be target produces fast neutrons with energy of above 10 keV. The flux of fast neutron increases as the energy of proton increases. The highest fast neutron flux is produced by interaction of 30 MeV protons with ^{9}Be target. The highest intensity of fast neutrons is in the vicinity of the target. The neutron flux spreads from the vicinity of the target to the DLBSA components. Based on the results of the optimization of the thickness and diameter of the target, it is found that the highest fast neutron flux was at the diameter of 7 cm and thickness of 5 cm with neutron flux of 4.26 x 10^{9} n/cm^{2}/s. The increase in the fast neutron flux produced by the target impacts the increase in the epithermal neutron flux produced by DLBSA.

Acknowledgment

The author expresses his gratitude to LPPM Unsoed, which has fully funded this research through the Unsoed Basic Research Grant with Contract Number 1068/UN23/HK02/2021.

Conflic of Interest. The authors declare they have no conflict of interest.

References

Anderson, I.S., Andreani, C., Carpenter, J.M., Festa, G., Gorini, G., Loong, C.K., Senesi, R. 2016. Research opportunities with compact accelerator driven neutron sources. *Physics Reports*, **654:** 1-58.

Bilalodin, B., Suparta, G.B., Hermanto, A., Palupi, D.S., Sardjono, Y., Rasito, R. 2020. Analysis of particle distribution in a double layer beam shaping assembly resulted from 30 MeV-proton reactions with beryllium target using The PHITS program. *Jurnal Teknologi*, **82:** 70-74.

Bilalodin, B., Suparta, G.B., Hermanto, A., Palupi, D.S., Sardjono, Y., Rasito, A. 2019. Characteristics of thermal neutron flux distribution in a phantom irradiated by epithermal neutron beam from double layer beam shaping assembly (DBSA). *Pakistan Journal of Scientific and Industrial Research Series A: Physical Sciences*, **62:** 167-173.

Capoulat, M.E., Herrera, M.S., Minsky, D.M., González, S.J., Kreiner, A.J. 2014. ^{9}Be(d,n)^{10}B based neutron sources for BNCT. *Applied Radiation and Isotopes*, **88:** 190-194.

Chavan, V., Ham, C., Bak, S.I., Gore, V., In, E.J., Moon, D., Hong, S.W. 2022. Monoenergetic neutrons from the ^{9}Be(p,n)^{9}B reaction induced by 35, 40 and 45-MeV protons. *Nuclear Physics A*, **1018:** 122-130.

Dymova, M.A., Taskaev, S.Y., Richter, V.A., Kuligina, E.V. 2020. Boron neutron capture therapy: current status and future perspectives. *Cancer Communications*, **40:** 406-421.

Faghihi, F., Khalili, S. 2013. Beam shaping assembly of a D-T neutron source for BNCT and its dosimetry simulation in deeply-seated tumor. *Radiation Physics and Chemistry*, **89:** 1-13.

Fantidis, J.G., Nicolaou, G. 2018. Optimization of beam shaping assembly design for boron neutron capture teraphy based on a tranportable proton accelerator. *Alexandria Eninering Journal*, **57:** 2333-2342.

Feghhi, S.A.H., Gholamzadeh, Z., Tenreiro, C. 2014. Investigation of the optimal material type and dimension for spallation targets using simulation methods. *Journal of Theoretical and Applied Physics*, **8:** 117-123. https://doi.org/10.1186/2251-72358-1

Hang, S., Tang, X., Shu, D., Liu, Y., Geng, C., Gong, C., Chen, D. 2016. Monte Carlo study of the beam shaping assembly optimization for providing high epithermal neutron flux for BNCT based on D–T neutron generator. *Journal of Radioanalytical and Nuclear Chemistry*, **310:** 1289-1298. https://doi.org/10.1007/s10967-016-5001-4

Hashimoto, Y., Hiraga, F., Kiyanagi, Y. 2014. Effects of proton energy on optimal moderator system and neutron induced radioactivity of compact accelerator-driven 9Be(p,n) neutron sources for BNCT. *Physics Procedia*, **60:** 332-340.

He, H., Li, J., Jiang, P., Tian, S., Wang, H., Fan, R., Wang, J. 2021. The basis and advances in clinical application of boron neutron capture therapy. *Radiation Oncology*, **16:** 1-8. https://doi.org/10.1186/s13014-021-01939-7

Iwamoto, H., Meigo, S.I., Matsuda, H. 2020. A comprehensive study of spallation models for proton-induced spallation product yields utilized in transport calculation. In: *Proceeding of EPJ Web of Conferences*, pp. 1-6, 1J-PARC Center, Japan Atomic Energy Agency, 2-4, Shirakata, Tokai-mura, Naka-gun, Ibaraki 319-1195, Japan. https://doi.org/10.1051/epjconf/202023906001

Koay, H.W., Fukuda, M., Toki, H., Seki, R., Kanda, H., Yorita, T. 2018. Feasibility study of compact accelerator based neutron generator for multi-port BNCT system. *Nuclear Instruments and Methods in Physics Research Section A*, **899:** 65-72.

Lee, S., Chang, H., Lee, J., Kye, Y.U., Ye, S.J. 2020. Neutron yields of ^{9}Be(p,xn) reactions and beam characterization for accelerator based boron neutron capture therapy facility using MCNP6, PHITS and GEANT4 simulation results. *Nuclear Instruments and Methods in Physics Research Section B*, **478:** 233-238.

Ma, C.W., Lv, C.J., Zhang, G.Q., Wang, H.W., Zuo, J.X. 2015. Neutron induced reactions on AlF3 studied using the optical model. *Nuclear Instruments and Methods in Physics Research Section B*, **356:** 42-45. https://doi.org/10.1007/s10967-016-5001-4

Mank, G., Bauer, G., Mulhauser, F. 2011. Accelerators for neutron generation and their applications. *Reviews of Accelerator Science and Technology*; *Accelerator Applications in Industry and the Environment*, **4:** 219-233. https:/doi.org/10.1142/S1793626811000549.

Sato, T., Niita, K., Matsuda, N., Hashimoto, S., Iwamoto, Y., Noda, S., Shihver, L. 2013. Particle and heavy ion transport system, PHITS, version 2.52. *Journal of Nuclear Science and Technology*, **50:** 913-922. https://doi.org/10.1080/00223131.2013.814553

Savolainen, S., Kortesniemi, M., Timonen, M., Reijonen, V., Kuusela, L., Uusi-Simola, J., Auterinen, I. 2013. Boron neutron capture therapy BNCT in Finland: technological and physical prospects after 20 years of experiences. *Physica Medica*, **293:** 233-248.

Shin, J.W., Park, T.S. 2015. New charge exchange model of GEANT4 for ^{9}Be(p,n)^{9}B reaction. *Nuclear Instruments and Methods in Physics Research Section B: Beam Interactions with Materials and Atoms*, **342:** 194-199.

Stefanik, M., Bem, P., Majerle, M., Novak, J., Simeckova, E., Stursa, J. 2019. Neutron field study of p(35)+Be source reaction at the NPI Rez. *Radiation Physics and Chemistry*, **155:** 294-298.

Tanaka, H., Sakurai, Y., Suzuki, M. 2011. Experimental verification of beam characteristics for cyclotron-based epithermal neutron source (C-BENS). *Applied Radiation and Isotopes*, **69:** 1642-1645.

Zaidi, L., Kashaeva, E.A., Lezhnin, S.I., Malyshkin, G.N., Samarin, S.I., Sycheva, T.V., Taskaev, S.V., Frolov, S.A. 2017. Neutron beam shaping assembly for boron neutron capture therapy, *Physics of Atomic Nuclei*, **80:** 60-66. https://doi.org/10.1134/S106377881701015X